Article

Structure-based enzyme tailoring of 5-hydroxymethylfurfural oxidase

Willem Pieter Dijkman, Claudia Binda, Marco W. Fraaije, and Andrea Mattevi

ACS Catal., **Just Accepted Manuscript** • DOI: 10.1021/acscatal.5b00031 • Publication Date (Web): 09 Feb 2015

Structure-based enzyme tailoring of 5-hydroxymethylfurfural oxidase

Willem P. Dijkman[†,§], *Claudia Binda*[‡,§], *Marco W. Fraaije*[†,*], *Andrea Mattevi*[‡,*]

[†]Molecular Enzymology group, Groningen Biomolecular Sciences and Biotechnology Institute, University of Groningen, Nijenborgh 4, 9747 AG, Groningen, The Netherlands

[‡]Dept. Biology and Biotechnology, University of Pavia, via Ferrata 1, 27100 Pavia, Italy

KEYWORDS:

5-hydroxymethylfurfural oxidase

enzyme

2,5-furandicarboxylic acid

biocatalysis

protein engineering

crystal structure

ABSTRACT

5-hydroxymethylfurfural oxidase (HMFO) is a flavin-dependent enzyme that catalyzes the oxidation of many aldehydes, primary alcohols, and thiols. The three-step conversion of 5-hydroxymethylfurfural to 2,5-furandicarboxylic acid is relevant for the industrial production of biobased polymers. The remarkable wide substrate scope of HMFO contrasts with the enzyme's precision in positioning the substrate to perform catalysis. We have solved the crystal structure of HMFO at 1.6 Å resolution, which guided mutagenesis experiments to probe the role of the active-site residues in catalysis. Mutations targeting two active-site residues generated engineered forms of HMFO with promising catalytic features, namely enantioselective activities on secondary alcohols and improved 2,5-furandicarboxylic acid yields.

INTRODUCTION

The enzyme 5-hydroxymethylfurfural oxidase from *Methylovorus* sp. strain MP688 (HMFO, EC 1.1.3.47) catalyzes the oxidation of 5-hydroxymethylfurfural (**1**) to 2,5-furandicarboxylic acid (**4**),[1] the latter can be esterified to form polymers with a wide variety of applications.[2,3] Because 5-hydroxymethylfurfural (**1**) can be derived from sugars, the enzyme is of particular interest for the production of bio-based plastic materials in an environmentally-friendly industrial process. The overall reaction consists of three oxidation steps and HMFO can performs all these steps as depicted in Scheme 1.[4] The alcohol group of 5-hydroxymethylfurfural (**1**) is first oxidized to the corresponding aldehyde to generate furan-2,5-dicarbaldehyde (**2**).[4] This compound undergoes spontaneous hydration to the *gem*-diol which is oxidized by the enzyme to 5-formyl-2-furancarboxylic acid (**3**). Finally, also this monocarboxylic intermediate product is released, non-enzymatically hydrated, and oxidized by HMFO to the dicarboxylic reaction product.[4] Importantly, the poor activity of HMFO towards 5-formyl-2-furancarboxylic acid (**3**) is limiting the efficiency of the overall process. Increasing the activity towards 5-formyl-2-furancarboxylic acid (**3**) is addressed in this study.

HMFO is a member of the glucose-methanol-choline (GMC) family of oxidoreductases.[1] HMFO, like other members of this enzyme family, relies on the presence of the flavin adenine dinucleotide (FAD) cofactor as prosthetic group and an active site histidine (H467 in HMFO) serving as base. This residue, which is conserved in all GMC enzymes,[5–10] initiates the reaction by removing the proton from the alcohol group of the substrate. The second step, taking place simultaneously with or after proton abstraction,[11–13] is the hydride transfer from the α-carbon of the substrate to the FAD N5 and thereby completing the oxidation reaction. This results in the reduced flavin which is reoxidized by molecular oxygen, yielding hydrogen peroxide as by-

product (Scheme 1). The active site histidine is crucial for catalysis, functioning as the main anchoring element for the alcohol group of the substrate.[1] The nature of this alcohol groups is very important as only primary alcohols, primary thiols, and aldehydes are oxidized by HMFO.[14] Secondary alcohols are not converted, indicating that the enzyme is very specific concerning the substrate type.[1] On the other hand, HMFO is strikingly promiscuous concerning the side chain next to the alcohol group. Most (but not all) of the identified substrates are aromatic, including furanic, phenylic and cinnamylic alcohols. Ring substituents with different size, polarity and charge are allowed in the active site of HMFO, both on the *para* and *meta* positions relative to the alcohol.[1]

To investigate how this biocatalyst can be so precise in accepting aldehydes, primary alcohols and thiols and yet so promiscuous concerning the rest of the substrate, we solved the HMFO crystal structure. The three-dimensional model provides the framework for protein engineering studies aimed at the generation of variants with interesting and improved biocatalytic properties. In particular, several HMFO mutants were designed and produced which display higher activities towards 5-formyl-2-furancarboxylic acid (**3**), thereby improving the enzymatic formation of 2,5-furandicarboxylic acid (**4**) from 5-hydroxymethylfurfural (**1**). In addition, mutant enzymes were designed which can enantioselectively convert secondary alcohols, an activity not found in the wild type enzyme.

MATERIALS AND METHODS

Purification of HMFO

For kinetic and spectral analysis, HMFO and its mutants were expressed as a N-terminal SUMO fusion protein in *Escherichia coli* BL21 (DE3) and purified using affinity chromatography as described before.[1] For structural characterization similar procedures were used in the first steps of HMFO purification, including affinity purification that was performed on a 5 mL HisTrap HP column using an Äkta Purifier system (GE Healthcare). In addition, tag cleavage was performed by incubating the eluted protein with 0.1 mg of SUMO protease (home-made) and dialyzing overnight at 4 °C against 50 mM Tris/HCl pH 7.5, 150 mM NaCl. The dialyzed sample was loaded again on a 5 mL HisTrap HP column to remove the tag and the SUMO protease. HMFO was eluted in the flow-through and then loaded on a Superdex200 16/60 (GE Healthcare) equilibrated with 50 mM potassium phosphate buffer pH 7.6. A single and sharp peak was obtained. Based on the retention time of HMFO and protein standards of known size, this is consistent with a monomeric homogeneous form of the protein. Fractions were pooled and concentrated with Amicon 30K (Millipore), yielding about 30 mg of pure protein (from 10 g of *E. coli* cells, wet weight).

Site directed mutagenesis

To introduce mutations into HMFO, a whole-plasmid PCR was performed. The primers used to introduce the mutations are listed in Table S1 of the supporting information. The template DNA was cleaved with DpnI (New England BioLabs) and the PCR-product was purified afterwards using a PCR purification kit (Qiagen). *E. coli* TOP10 cells were transformed with the plasmids and the introduction of the mutation was confirmed by sequencing.

Product formation by mutant enzymes V367 and W466 and V367R-W466F

2,5-Furandicarboxylic acid (**4**) generation by wild type HMFO and the mutant enzymes V367K, V367R, W466F and W466A or the double mutant enzyme V367R-W466F was assayed by using 2.0 μM or 20 μM enzyme with 5.0 mM 5-hydroxymethylfurfural (**1**) or 5-formyl-2-furancarboxylic acid (**3**) in a 100 mM potassium phosphate buffer of pH 7.0 (25 °C, 1000 RPM). The reaction was stopped by heating the mixture at 70 °C. Subsequent centrifugation (5 minutes at 13000 × g) was used to remove the denatured enzyme. The products formed were analyzed by HPLC, as described elsewhere.[1]

Kinetic analysis

Steady state parameters for HMFO wild type and HMFO mutants were obtained by monitoring the conversion of 4-hydroxy-3-methoxybenzyl alcohol (vanillyl alcohol). Formation of the product, 4-hydroxy-3-methoxybenzaldehyde (vanillin), was measured at 340 nm (ε_{340} = 14 mM^{-1} cm^{-1}) using between 0.10 and 4.2 μM enzyme, depending on the HMFO variant, while varying the substrate concentration between 0.01 and 40 mM. All kinetic experiments were performed at atmospheric oxygen conditions. The assay was performed in a 50 mM Tris/HCl buffer pH 7.5 at 25 °C. To determine the steady state parameters of HMFO V367R, W466F and V367R-W466F on 5-formyl-2-furancarboxylic acid (**3**) (TCI Europe), oxygen depletion was measured as described elsewhere.[1] The observed rates were fitted with Michaelis-Menten kinetics equation, $v = (k_{cat\ (app)} \cdot [S])/((K_{M\ (app)} + [S])$ or with an equation taking substrate inhibition into account, $v = (k_{cat\ (app)} \cdot [S]/(K_{M\ (app)} + [S] \cdot (1 + [S]/K_{i\ (app)}))$. To determine the $k_{cat\ (app)}/K_{M\ (app)}$ values for wild-type and mutant HMFO on 5-formyl-2-furancarboxylic acid (**3**), the oxidation of 0.056 up to 4.0 mM substrate was followed at 310 nm (ε_{310} = 2.5 mM^{-1} cm^{-1}) for 60 minutes in a 50 mM potassium phosphate buffer of pH 8.0. The slope of the linear relation between the observed rate

and the concentration of 5-formyl-2-furancarboxylic acid (**3**) was taken as the $k_{cat\ (app)}/K_{M\ (app)}$ value.

Activity towards secondary alcohols

The activity of HMFO wild type and mutant enzymes towards the secondary alcohols *S*-1-phenylethanol and *R*-1-phenylethanol (both Sigma Aldrich) was assayed by incubating 5.0 μM enzyme with 5.0 mM substrate, the reaction was monitored for 50 minutes. Control reactions without enzyme or without substrate were also performed. Steady state kinetics of the HMFO W466F and W466A mutants (5 μM) were obtained using between 0.05 to 50 mM *S*-1-phenylethanol. 1-Phenylethanol conversion was measured by the formation of the product, acetophenone, at 247 nm (ε_{247} = 10.8 mM^{-1} cm^{-1}). Experiments were performed in a 50 mM potassium phosphate buffer of pH 8.0 at 25 °C at atmospheric oxygen concentrations.

Crystallization and structure determination

Pure HMFO (both wild type and H467A mutant, 10 mg/mL in 50 mM potassium phosphate buffer pH 7.6) was crystallized using the hanging-drop vapor diffusion method by mixing 1.0 μl of protein with 1.5 μl of a reservoir solution containing 16-22% w/v PEG3350 and 200 mM magnesium formate. Yellow flat crystals grew in 2-5 days at 20 °C. For X-ray data collection crystals were soaked in a cryosolution consisting of 26% w/v PEG3350, 200 mM magnesium formate, 15% v/v glycerol and flash-cooled in liquid nitrogen. For the structural characterization of enzyme-substrate complexes, crystals were soaked in cryosolutions containing different substrates (5-hydroxymethylfurfural, vanillyl alcohol, (2E)-3-phenylprop-2-en-1-ol (cinnamyl alcohol), furan-2,5-dicarbaldehyde, phenylmethanethiol, (4-nitrophenyl)methanethiol or

terephthalaldehyde) using different concentrations depending on compound solubility. Bleaching of the yellow color of the crystal, indicative for flavin reduction, was monitored under the microscope followed by flash-cooling in liquid nitrogen. In the case of the catalytically-inactive H467A mutant enzyme, co-crystallization with 10 mM 5-hydroxymethylfurfural was also carried out. X-ray data collection was performed at the beamlines ID23-EH1 (ESRF, Grenoble, France), X06SA (SLS, Villigen, Switzerland) and P13 (DESY-PETRAIII, Hamburg, Germany). Data processing and scaling were performed using MOSFLM[15] and programs of the CCP4 package.[16] The HMFO structure was initially solved by molecular replacement using the program BALBES[17] which selected choline oxidase as the best starting model (PDB code = 4MJW; 31% sequence identity). Model building and structure analysis were performed by the program COOT,[18] whereas refinement was carried out by REFMAC5.[19] Data collection and refinement statistics are reported in Table S2. Figures were created by CCP4mg.[20] Atomic coordinates and structure factors were deposited with the Protein Data Bank (codes 4UDP, 4UDQ, 4UDR).

RESULTS AND DISCUSSION

Three structures of the enzyme, the wild type in its oxidized and reduced forms and a mutant enzyme (HMFO H467A), were solved at 1.6-1.9 Å resolution (Figures 1A and S1; Table S2). Out of the 531 residues of HMFO, only the four N-terminal and two C-terminal amino acids lack clear electron density whereas loop 326-330 is poorly ordered in the oxidized enzyme. Though being monomeric in solution, the two HMFO molecules present in the asymmetric unit form a dimer that involves a limited interface area with no catalytically relevant regions (less than 4% of the total protein surface). Comparison with other proteins of the GMC family

revealed that choline oxidase,[21] pyridoxine-4-oxidase[22] and aryl-alcohol oxidase[23] have the most similar structural architecture to HMFO (rmsd calculated on the Cα positions is 2.0, 2.1 and 2.2 Å, respectively), followed by glucose oxidase[24] (rmsd of 2.3 Å) and pyranose-2-oxidase[25] (rmsd of 3.0 Å). Choline oxidase and glucose oxidase have dimeric structures, which, unlike HMFO, are essential for their catalytic activity and involve about 10% of their monomer surface.

The 531 HMFO residues fold into a globular and compact structure organized in two domains: the FAD-binding domain (residues 5-158, 208-307, 372-402, 466-529), characterized by the typical Rossmann fold topology that embeds the non-covalently bound FAD cofactor, and a smaller cap domain (residues 159-207, 308-371, 403-465) that covers the flavin site. Some oxidases of the GMC family, like choline oxidase and pyranose-2-oxidase, contain a covalently bound FAD cofactor, linked via a 8α-N3-histidyl bond. In HMFO, V101 replaces the histidine present in these enzymes. Mutagenesis experiments show that introducing a histidine in HMFO does not result in a covalently bound cofactor and renders the enzyme inactive, possibly because the imidazole ring interferes with proper positioning of the FAD cofactor (Table S3). Only with the double mutant enzyme HMFO F67V-V101H, designed to leave space for the histidine side chain, some activity was observed but again, the covalent link was not formed.

At the interface between the FAD and the cap domains of HMFO, a deep and narrow cleft is formed which represents the enzyme active site (Figure 1B). The flavin ring and the side chain of H467 are positioned at the bottom of this cleft. The latter residue is strictly conserved in the oxidases of the GMC family and was shown to be essential for catalysis by functioning as both active site base and H-bond acceptor for the substrate OH group.[1] As anticipated, the H467A mutant enzyme is catalytically almost inactive (activity decrease by >3 orders of magnitude, see Table 1) and the elucidation of its crystal structure showed that the mutation does not result in

any conformational change (the overall rmsd for the Cα atoms with respect to the wild type protein is 0.39 Å) apart from the binding of three additional water molecules that replace the H467 side chain (Figure S1). Together with H467, N511 forms a hydrogen-bond dyad for the substrate. N511 is a conserved residue in several GMC type oxidases, and removal of the side chain in the N511A mutant enzyme reduces catalysis, although the effect is much smaller compared to the H467A mutant enzyme (Table 1). Apart from these two residues, the HMFO active site is quite hydrophobic (Figure 2). Many attempts were made to obtain the structure of HMFO in complex with either substrate or product by soaking crystals in a mother liquor containing a ligand. By monitoring the bleaching of the yellow color of the crystal (indicating the reduction of the FAD cofactor), we were able to obtain crystals of HMFO in the reduced state. The elucidated structure of the reduced enzyme was essentially indistinguishable from that of the oxidized protein. Moreover, in the substrate reduced enzyme crystals, we could not observe electron density indicating the presence of any ligand. This might be related to the architecture of the HMFO active site cleft, characterized by its free entrance (Figure 1B). Other GMC oxidases also feature a narrow channel for substrate binding, but in these enzymes the active site is more buried and the access to it is often gated by conformational changes of specific loops.[22,23,26,27]

A combination of modeling and mutagenesis experiments were performed to gain insights into the role of several residues in substrate binding. On the basis of the constraints imposed by the position of the Cα-H oxidation site towards the FAD cofactor and the hydroxyl group interaction with H467,[28] we modeled the 5-hydroxymethylfurfural (**1**) molecule in the enzyme active center (Figure 3A). The shape of the cleft constrains the furan ring (as well as the aromatic moiety of vanillyl alcohol, not shown) in a unique conformation, squeezed by the hydrophobic residues surrounding the active site (Figure 2). To investigate this aspect, residues M103, W369, F434,

V465 and W466 were mutated to alanine and the steady state kinetics of the mutant enzymes were studied using vanillyl alcohol as a model substrate (Table 1). The most pronounced effects are observed in the case of the HMFO M103A, W369A, V465A and W466A mutants. These residues are close to the active site base H467 and their removal creates a large space which likely affects the proper orientation of the substrate with respect to the flavin. In addition, W466 is in close proximity of the flavin ring (Figure 2) and, consistently, removal of this side chain turns out to affect protein stability (Tables S4). F434 is further away from the oxidation site and the effect on catalysis of F434A is smaller compared to the mutant enzymes described above. The overall picture emerging from these experiments is that the active site funnel is designed to create a sterically restrained site that positions the reactive primary alcohol of the substrate in the proper H-bonding environment and geometric relation with the flavin to promote catalysis.

Along this line, we reasoned that some of the created mutant enzymes, though less efficient on primary alcohols, could instead become active on bulkier secondary alcohols as consequence of an enlarged the active site cleft. Consistently, the W466F and W466A were found to be active on *S*-1-phenylethanol, with W466A performing best (Table 2). Remarkably, the W466 mutant enzymes are strictly enantioselective as they have no activity on *R*-1-phenylethanol (Table S5), similar to the results for the analogues mutation in the fungal aryl-alcohol oxidase.[29] These data are in full agreement with the structural modelling of 1-phenylethanol in HMFO because the *R*-enantiomer would not bind with the Cα hydrogen pointing towards the flavin N5 as requested for oxidation. The *S*-enantiomer, on the other hand, would have its methyl group colliding with the W466 side chain, a problem which is overcome by the W466F or W466A mutations (Figure 3B).

The rate limiting step in the HMFO catalyzed oxidation of 5-hydroxymethylfurfural (**1**) to 2,5-furandicarboxylic acid (**4**) is the oxidation of 5-formyl-2-furancarboxylic acid (**3**) (Scheme 1).[4]

Therefore, increasing the rate of catalysis for this last oxidation step would lead to higher product yields. These thoughts led us to analyze the activity of some of the mutant enzymes towards aldehyde substrates, which have to be in their *gem*-diol form in order to be converted by HMFO. Indeed, both secondary alcohols and *gem*-diols have bulky substituents on the α-carbon compared to primary alcohols. Therefore, although less active on primary alcohols (Table S6), the W466F and W466A mutants were tested against the aldehyde 5-formyl-2-furancarboxylic acid (**3**), both showing increased activity with a noticeable conversion of 49% of 5-formyl-2-furancarboxylic acid (**3**) into 2,5-furandicarboxylic acid (**4**) in 24 hours (three times more than the wild type enzyme; Table S6). With these studies W466 was identified as a valuable target site for mutants featuring improved activity on aldehyde substrates by creating a more spacious binding cleft for a *gem*-diol substrate.

Both furanic and phenylic substrates with a negatively charged carboxylic acid on the *para* position are much less efficiently converted than their non-charged analogues.[1,4] This poor activity of wild type HMFO towards for instance 5-formyl-2-furancarboxylic acid (**3**) is likely due to a high $K_{M\ (app)}$ value (Table 2). Similar results were described recently for aryl-alcohol oxidase. This enzyme cannot perform the three oxidations required to form 2,5-furandicarboxylic acid (**4**) from 5-hydroxymethylfurfural (**1**), as it is not active towards 5-formyl-2-furancarboxylic acid (**3**).[30] To improve activity of HMFO for 5-formyl-2-furancarboxylic acid (**3**), V367 represents a candidate for mutagenesis (see Figure 3A). Two HMFO mutants, V367K and V367R, were produced and characterized. It was gratifying to observe that both enzyme variants showed significantly improved activity towards 5-formyl-2-furancarboxylic acid (**3**) (Table S6). In particular, V367R is able to form 97% of 2,5-furandicarboxylic acid (**4**) in 6 hours, whereas the wild type enzyme needs 24 hours to reach 92% conversion. This can also be seen from the

amounts of catalyst needed to obtain 50% conversion: the V367R mutant enzyme outperforms the wild type protein by reaching similar product quantities in 12 hours with 10 times less biocatalyst (Table S6). Similar results are obtained when the entire reaction is tested, *i.e.* using 5-hydroxymethylfurfural (**1**) as initial substrate (Table S6). Clearly, HMFO V367R results in a better 5-hydroxymethylfurfural (**1**) to 2,5-furandicarboxylic acid (**4**) conversion (~3 fold higher). These data demonstrate that the introduction of a positive charge at this side of the active site increases the activity towards 5-formyl-2-furancarboxylic acid (**3**) by helping to position the substrate.

These mutagenesis experiments identified W466 as site for mutations increasing activities on the aldehyde 5-formyl-2-furancarboxylic acid (**3**) and V367 as a site for improving the activity on carboxylic acid-containing substrates. A logical continuation was to evaluate the effect of the combined mutations. The V367R-W466F double mutant was constructed and tested for its activity towards 5-formyl-2-furancarboxylic acid (**3**). The double mutant enzymes has an almost tenfold higher $k_{cat\ (app)}$ when compared to the individual single mutant enzymes and also the lowest $K_{M\ (app)}$ value (Table 2), resulting in a catalytic efficiency (k_{cat}/K_M) for 5-formyl-2-furancarboxylic acid (**3**) which is over 1000 fold higher than wild type HMFO. HPLC analysis confirms the double mutant is superior to both the single mutants and wild type HMFO for the formation of 2,5-furandicarboxylic acid (**4**) (Table S6). Moreover, the double mutant displayed enhanced efficiency in the overall conversion 5-hydroxymethylfurfural (**1**) to 2,5-furandicarboxylic acid (**4**), a feature of self-evident relevance for the biotechnological applications of the enzyme.

CONCLUSIONS

An intriguing aspect of HMFO is its dual character of being very precise in the oxidation of primary alcohols (*i.e.* devoid of any activity on secondary alcohols) and at the same time so promiscuous in converting a broad range of primary alcohols. At the heart of this feature is an active-site cleft which provides an essential H-bonding anchoring point that activates the substrate and positions the substrate α-carbon in direct contact with the flavin. The crystal structure shows that a constellation of mostly hydrophobic amino acids shapes the active site clef to make it selective for aromatic and aliphatic primary alcohols. This active site architecture is amenable to protein engineering to design biocatalysts with enhanced activities towards substrates with varying bulkiness and electrostatic properties. In particular, it was possible to identify mutant enzyms that are active on secondary alcohols, with the added value that their enantioselectivity can be used for kinetic resolution of chiral secondary alcohols.[31–33] Equally valuable, mutant enzymes were created with increased activity towards the intermediates formed during the multistep HMFO-mediated production of 2,5-furandicarboxylic acid (**4**). These properties culminate in a double mutant that combines the best of these individual mutant enzymes, having the highest turnover number and affinity for 5-formyl-2-furancarboxylic acid (**3**), leading to the highest 2,5-furandicarboxylic acid (**4**) yield. All these findings will guide further investigations on HMFO catalytic activities and will be valuable for industries focused on green chemistry approaches for bio-based plastics production.

FIGURES

Figure 1. The three-dimensional structure of HMFO.

A

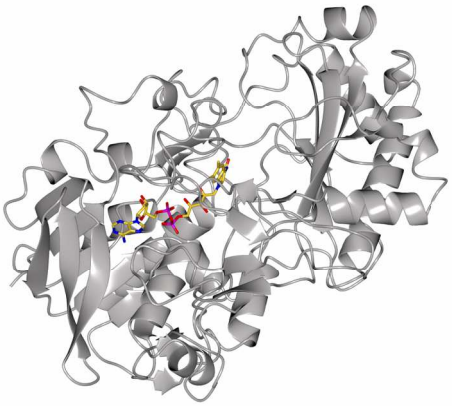

B

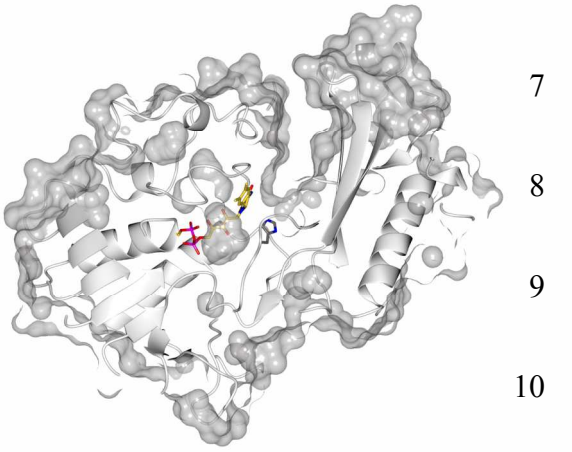

(A) Ribbon diagram of the overall structure with its FAD cofactor bound (represented with carbon, oxygen, nitrogen and phosphor atoms in yellow, red, blue and magenta). (B) HMFO surface highlighting the active site cleft that is about 20 Å deep and on average 10 Å large (the representation was front- and back-clipped to make the cleft space visible). In front of the flavin ring the side chain of the conserved His467 is at the bottom of the active site.

Figure 2. Stereo view of the active site of HMFO (reduced state).

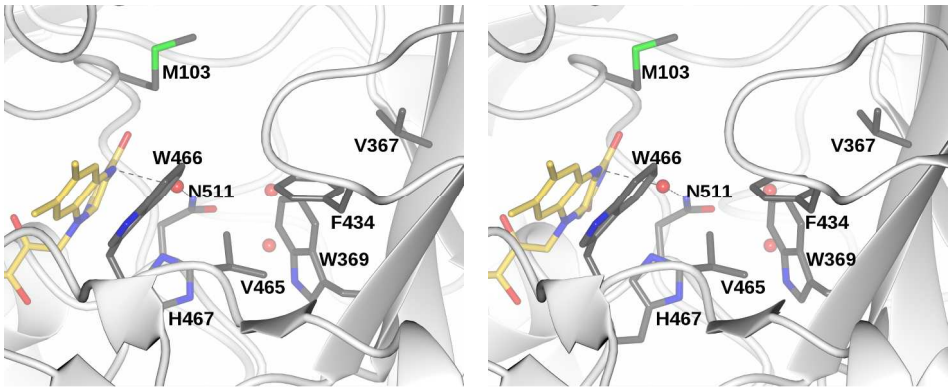

Residues surrounding the space in front of the flavin ring are shown, including three water molecules (red spheres) that are conserved in all determined HMFO crystal structures (only one is missing in the oxidized enzyme, which may be related to the lower resolution). Color coding is as in Figure 1 (sulfur atoms in green). Hydrogen bonds are represented as dashed lines.

Figure 3. Modeling of substrate binding in HMFO active site.

A

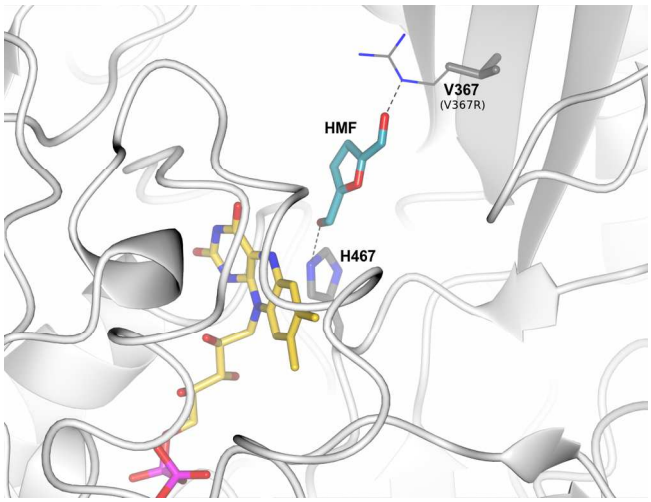

B

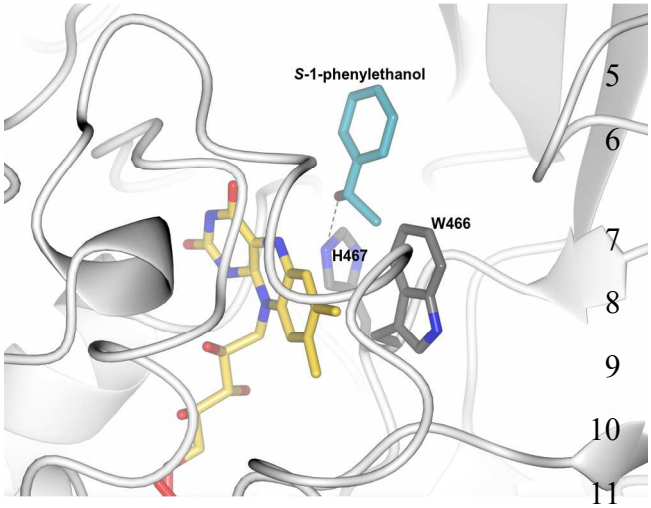

(A) Proposed model for the binding of 5-hydroxymethylfurfural substrate (**1**). The furan ring orientation is constrained by the narrow shape of the cleft and the substrate α-carbon is in the proper position to be oxidized by the flavin.[28] The protein atom closest to the substrate hydroxyl group is Nε2 of His467, which is perfectly positioned to form a H-bond with the substrate. The orientation of the His467 imidazole ring was assigned on the basis of a favorable H-bond interaction between its Nδ1 atom and the neighboring His307 side chain (not shown for clarity).

The arginine side chain of the V367R mutant was modeled to show the possible interaction with the substrate, which would provide an explanation for the increased activity of this mutant with 5-formyl-2-furancarboxylic acid (**3**) (Table 2). (B) Similarly to 5-hydroxymethylfurfural (**1**), the secondary alcohol *S*-1-phenylethanol was modeled in HMFO active site. The model is consistent with the biochemical data showing that wild type HMFO is not able to oxidize this substrate because the substrate methyl group would collide with W466 side chain. According to the model, the smallest distance between the methyl group of *S*-1-phenylethanol and W466 is 2.3 Å.

SCHEMES

Scheme 1. The oxidation of 5-hydroxymethylfurfural (**1**) to 2,5-furandicarboxylic acid (**4**) by HMFO.

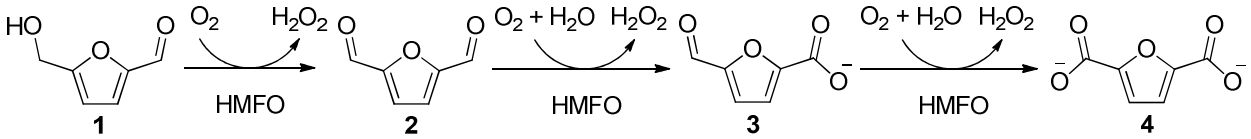

Conversion of **1** to **4** is initiated by oxidation of the alcohol group of **1**, resulting in furan-2,5-dicarbaldehyde (**2**). The hydrated form of **2** is converted to 5-formyl-2-furancarboxylic acid (**3**). The last step is the oxidation of the hydrated form of **3**, yielding **4**.

TABLES.

Table 1. Steady state parameters of the different HMFO variants on vanillyl alcohol [a]

Enzyme	$k_{cat\ (app)}$ (s^{-1})	$K_{M\ (app)}$ (mM)	$k_{cat\ (app)}/K_{M\ (app)}$ (s^{-1} mM^{-1})
Wild type	21 ± 0.42	0.72 ± 0.066	29
M103A	3.3 ± 0.051	1.8 ± 0.11	1.8
W369A	4.3 ± 0.0063	1.1 ± 0.067	3.9
F434A	15 ± 0.68	1.2 ± 0.23	12
V465A	1.5 ± 0.058	0.92 ± 0.16	1.6
V367K	5.1 ± 0.11	0.29 ± 0.032	18
V367R	6.0 ± 0.12	0.28 ± 0.027	21
W466F	1.7 ± 0.043	0.20 ± 0.027	8.5
W466A	0.75 ± 0.025	1.0 ± 0.15	0.75
H467A [b]	0.0047 ± 0.00023	0.82 ± 0.18	0.0057
N511A	1.0 ± 0.014	2.0 ± 0.10	0.55

[a] Experiments performed at 25 °C, in 50 mM Tris/HCl buffer of pH 7.5 at atmospheric oxygen concentration. Product formation was measured at 340 nm.

[b] Data published elsewhere.[1]

Table 2. Steady state parameters of the engineered HMFO variants[a]

Enzyme		$k_{cat\ (app)}$ (s^{-1})	$K_{M\ (app)}$ (mM)	$k_{cat\ (app)}/K_{M\ (app)}$ (s^{-1} mM^{-1})
wild type	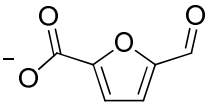	n.s.[b]	> 4.0	0.0005
V367R[c]		0.056	1.4	0.041
W466F		0.079	3.0	0.026
V367R-W466F[c]		0.46	0.21	2.2
wild type	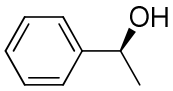	n.d.[d]	n.d.	n.d.
W466A		0.011	20	$0.55 \cdot 10^{-3}$
W466F		0.010	98	$0.10 \cdot 10^{-3}$

[a] The activity of HMFO variants towards 5-formyl-2-furancarboxylic acid (**3**) was measured using O_2 depletion whereas the activity towards *S*-1-phenylethanol was measured by the formation of product at 247 nm (ε_{247} = 10.8 mM^{-1} cm^{-1}) in a 50 mM potassium phosphate buffer of pH 8.0 at 25 °C at atmospheric oxygen concentration.

[b] n.s. = no saturation. Activity of HMFO at saturated substrate conditions could not be measured, preveting estimation of the $k_{cat\ (app)}$. The $k_{cat\ (app)}/K_{M\ (app)}$ value for wild type HMFO was determined by measuring the decrease of 5-formyl-2-furancarboxylic acid (**3**) (ε_{310} = 3.7 mM^{-1} cm^{-1}) at low concentration of 5-formyl-2-furancarboxylic acid (**3**) (≤ 4.0 mM), where the linear relation between the rates (s^{-1}) and the substrate concentration (mM) represents the $k_{cat\ (app)}/K_{M\ (app)}$.

[c] Both HMFO V367R and V367R-W466F show substrate inhibition, with a $K_{i\ (app)}$ of 76 mM and 7.3 mM respectively.

[d] n.d. = not detectable. No activity can be detected towards *S*-1-phenylethanol using wild type HMFO.

ASSOCIATED CONTENT

Supporting Information. Primers used for the generation of the mutant enzymes (Table S1), electron density showing the H467A mutation in the crystal structure (Figure S1), Data collection and refinement statistics for HMFO, oxidized and reduced, and HMFO H467A (Table S2), steady state kinetics of HMFO V101H mutants (Table S3), spectral properties and apparent melting temperatures of all HMFO mutants (Table S4), activity towards secondary alcohols (Table S5), data on 5-hydroxymethylfurfural (**1**) and 5-formyl-2-furancarboxylic acid (**3**) conversion using different experimental conditions and HMFO mutant enzymes (Table S6).

AUTHOR INFORMATION

Corresponding Author

*E-mail: m.w.fraaije@rug.nl; andrea.mattevi@unipv.it

Author Contributions

The manuscript was written through contributions of all authors. All authors have given approval to the final version of the manuscript. [§]WPD and CB contributed equally.

Funding Sources

This work was carried out within the BE-Basic R&D Program, for which an FES subsidy was granted from the Dutch Ministry of Economic Affairs, Agriculture, and Innovation (EL&I).

ACKNOWLEDGMENT

We thank the European Synchrotron Radiation Facility (ESRF), the Swiss Light Source (SLS) and the Deutsches Elektronen-Synchrotron (DESY-PETRAIII) for providing beamtime and

assistance. We thank also the BioStruct-X program (project n. 5275) for funding synchrotron trips.

ABBREVIATIONS

HMFO, 5-hydroxymethylfurfural oxidase; GMC, glucose-methanol-choline; FAD, flavin adenine dinucleotide.

REFERENCES

(1) Dijkman, W. P.; Fraaije, M. W. *Appl. Environ. Microbiol.* **2014**, *80*, 1082–1090.

(2) Jong, E. de; Dam, M. A.; Sipos G J; Gruter, M. In *Biobased Monomers, Polymers, and Materials*; American Chemical Society, **2012**; 1–13.

(3) Kamm, B. *Angew. Chem. Int. Ed. Engl.* **2007**, *46*, 5056–5058.

(4) Dijkman, W. P.; Groothuis, D. E.; Fraaije, M. W. *Angew. Chem. Int. Ed. Engl.* **2014**, *53*, 6515–6518.

(5) Romero, E.; Gadda, G. *Biomol. Concepts* **2014**, *5*, 299–318.

(6) Smitherman, C. L.; Rungsrisuriyachai, K.; Germann, M. W.; Gadda, G. *Biochemistry* **2014**.

(7) Mugo, A. N.; Kobayashi, J.; Yamasaki, T.; Mikami, B.; Ohnishi, K.; Yoshikane, Y.; Yagi, T. *Biochim. Biophys. Acta* **2013**, *1834*, 953–963.

(8) Yue, Q. K.; Kass, I. J.; Sampson, N. S.; Vrielink, A. *Biochemistry* **1999**, *38*, 4277–4286.

(9) Wongnate, T.; Sucharitakul, J.; Chaiyen, P. *Chembiochem* **2011**, *12*, 2577–2586.

(10) Hernández-Ortega, A.; Lucas, F.; Ferreira, P.; Medina, M.; Guallar, V.; Martínez, A. T. *Biochemistry* **2012**, *51*, 6595–6608.

(11) Fan, F.; Gadda, G. *J. Am. Chem. Soc.* **2005**, *127*, 2067–2074.

(12) Hernández-Ortega, A.; Borrelli, K.; Ferreira, P.; Medina, M.; Martínez, A. T.; Guallar, V. *Biochem. J.* **2011**, *436*, 341–350.

(13) Wongnate, T.; Chaiyen, P. *FEBS J.* **2013**, *280*, 3009–3027.

(14) Ewing, T. A.; Dijkman, W. P.; Vervoort, J. M.; Fraaije, M. W.; van Berkel, W. J. H. *Angew. Chem. Int. Ed. Engl.* **2014**, *53*, 13206–13209.

(15) Battye, T. G. G.; Kontogiannis, L.; Johnson, O.; Powell, H. R.; Leslie, A. G. W. *Acta Crystallogr. D. Biol. Crystallogr.* **2011**, *67*, 271–281.

(16) Winn, M. D.; Ballard, C. C.; Cowtan, K. D.; Dodson, E. J.; Emsley, P.; Evans, P. R.; Keegan, R. M.; Krissinel, E. B.; Leslie, A. G. W.; McCoy, A.; McNicholas, S. J.; Murshudov, G. N.; Pannu, N. S.; Potterton, E. a; Powell, H. R.; Read, R. J.; Vagin, A.; Wilson, K. S. *Acta Crystallogr. D. Biol. Crystallogr.* **2011**, *67*, 235–242.

(17) Long, F.; Vagin, A. a; Young, P.; Murshudov, G. N. *Acta Crystallogr. D. Biol. Crystallogr.* **2008**, *64*, 125–132.

(18) Emsley, P.; Cowtan, K. D. *Acta Crystallogr. D. Biol. Crystallogr.* **2004**, *60*, 2126–2132.

(19) Murshudov, G. N.; Vagin, a a; Dodson, E. J. *Acta Crystallogr. D. Biol. Crystallogr.* **1997**, *53*, 240–255.

(20) McNicholas, S.; Potterton, E.; Wilson, K. S.; Noble, M. E. M. *Acta Crystallogr. D. Biol. Crystallogr.* **2011**, *67*, 386–394.

(21) Quaye, O.; Cowins, S.; Gadda, G. *J. Biol. Chem.* **2009**, *284*, 16990–16997.

(22) Mugo, A. N.; Kobayashi, J.; Mikami, B.; Ohnishi, K.; Yagi, T. *Acta Crystallogr. Sect. F. Struct. Biol. Cryst. Commun.* **2012**, *68*, 66–68.

(23) Fernández, I. S.; Ruíz-Dueñas, F. J.; Santillana, E.; Ferreira, P.; Martínez, M. J.; Martínez, A. T.; Romero, A. *Acta Crystallogr. D. Biol. Crystallogr.* **2009**, *65*, 1196–1205.

(24) Hecht, H.-J.; Kalisz, H. M.; Hendle, J.; Schmid, R. D.; Schomburg, D. *J. Mol. Biol.* **1993**, *229*, 153–172.

(25) Hallberg, B. M.; Leitner, C.; Haltrich, D.; Divne, C. *J. Mol. Biol.* **2004**, *341*, 781–796.

(26) Spadiut, O.; Tan, T.-C.; Pisanelli, I.; Haltrich, D.; Divne, C. *FEBS J.* **2010**, *277*, 2892–2909.

(27) Quaye, O.; Lountos, G. T.; Fan, F.; Orville, A. M.; Gadda, G. *Biochemistry* **2008**, *47*, 243–256.

(28) Fraaije, M. W.; Mattevi, a. *Trends Biochem. Sci.* **2000**, *25*, 126–132.

(29) Hernández-Ortega, A.; Ferreira, P.; Merino, P.; Medina, M.; Guallar, V.; Martínez, A. T. *Chembiochem* **2012**, *13*, 427–435.

(30) Carro, J.; Ferreira, P.; Rodríguez, L.; Prieto, A.; Serrano, A.; Balcells, B.; Ardá, A.; Jiménez-Barbero, J.; Gutiérrez, A.; Ullrich, R.; Hofrichter, M.; Martínez, A. T. *FEBS J.* **2014**, 10.1111/febs.13177.

(31) Turner, N. J. *Chem. Rev.* **2011**, *111*, 4073–4087.

(32) O'Reilly, E.; Iglesias, C.; Ghislieri, D.; Hopwood, J.; Galman, J. L.; Lloyd, R. C.; Turner, N. J. *Angew. Chem. Int. Ed. Engl.* **2014**, *53*, 2447–2450.

(33) Escalettes, F.; Turner, N. J. *Chembiochem* **2008**, *9*, 857–860.

Table of contents and abstract graphics